

See discussions, stats, and author profiles for this publication at: <https://www.researchgate.net/publication/6938280>

# Multiple Alignment Tensors from a Denatured Protein

ARTICLE *in* JOURNAL OF THE AMERICAN CHEMICAL SOCIETY · AUGUST 2006

Impact Factor: 12.11 · DOI: 10.1021/ja0627693 · Source: PubMed

---

CITATIONS

4

---

READS

19

4 AUTHORS, INCLUDING:



Ke Ruan

University of Science and Technology of China

10 PUBLICATIONS 228 CITATIONS

SEE PROFILE



Joel R Tolman

Johns Hopkins University

39 PUBLICATIONS 2,628 CITATIONS

SEE PROFILE

## Multiple Alignment Tensors from a Denatured Protein

Erika B. Gebel, Ke Ruan, Joel R. Tolman, and David Shortle\*

*Department of Biological Chemistry, Johns Hopkins University, School of Medicine, 1915 East Madison, Baltimore, Maryland 21205, and Department of Chemistry, Johns Hopkins University, 3400 North Charles Street, Baltimore, Maryland 21218*

Received April 20, 2006; E-mail: shortle@jhmi.edu

NMR spectroscopy has been shown to be useful in the study of denatured proteins, although the amount of structural information is limited by the absence of long-range NOEs. In recent years, large residual dipolar couplings (RDCs) from denatured proteins have been observed under alignment conditions produced by bicelles and strained polyacrylamide gels.<sup>1–4</sup> Unlike theoretical predictions based upon a random coil conformation,<sup>5</sup> denatured proteins display surprisingly variable couplings as a function of position along the chain, suggesting that residual structure is present. In the case of staphylococcal nuclease, the structure of the denatured state in buffer ( $\Delta 131\Delta$ ) has been determined to have a nativelike topology by over 600 distance measurements based on paramagnetic relaxation enhancement from 14 spin labels.<sup>6</sup> This observation, in combination with a highly significant correlation between RDCs in buffer and in 8 M urea, led to the conclusion that a nativelike topology persists in this denatured protein, even under strongly denaturing conditions.<sup>1</sup>

Denatured proteins, unlike native proteins, show a skewing of RDCs to one sign, a trend that becomes more pronounced as denaturing conditions become more severe.<sup>1</sup> Several explanations for this skewing have been proposed in the literature, such as (1) segments of extended or polyproline II secondary structure that align independently<sup>4</sup> or (2) enrichment of extended and polyproline II  $\phi/\psi$  values along the long molecular axis. In two recently published reports, very simple computational models were able to correctly predict some of the position-dependent variations in RDC profiles for several denatured proteins.<sup>7,8</sup> The success of such models suggests that a single set of RDCs obtained from a single alignment tensor may contain a rather limited amount of information and therefore does not necessarily report on the presence of significant long-range structure in denatured proteins.

In this report, we describe efforts to extend our picture of the residual structure in denatured nuclease by measuring RDCs with multiple alignment tensors. The residual dipolar interaction tensor corresponding to each NH bond requires five parameters for its specification.<sup>9,10</sup> If RDC datasets can be acquired encompassing five independent alignment conditions, it is possible to determine all five elements of the residual dipolar coupling tensor for each NH bond.<sup>11</sup> These tensors contain information about the orientational probability distribution for each bond and are usually rendered into a specific description of mean bond orientation, generalized order parameters, and motional asymmetry parameters. The challenge to obtain multiple alignments from denatured proteins is the seeming insensitivity of RDCs to different alignment conditions. As initial attempts to alter  $\Delta 131\Delta$ 's alignment with highly charged gels gave ambiguous results, the new method based on composite phage/polyacrylamide gels developed by Ruan and Tolman<sup>12</sup> was applied to denatured nuclease. This method involves the immobilization of Pf1 bacteriophage at varying angles relative to the cylinder axis of polyacrylamide gels, which are then stretched prior

**Table 1.** Orthogonal Linear Combination Data Set Values and Results of Deletion Validation Method

OLC	SV <sup>a</sup>	$\ D\ $ <sup>b</sup>	error( $\sigma$ )	RMSD <sup>c</sup>	$Q^*$ <sup>d</sup>	RMSD(j) max <sup>e</sup>	$Q^*(\text{max})$ <sup>f</sup>
1	112	6.21	0.112	0.123	0.020	0.174	0.028
2	11.9	0.66	0.104	0.073	0.111	0.103	0.157
3	5.14	0.28	0.096	0.077	0.284	0.162	0.570
4	3.76	0.21	0.113	0.086	0.416	0.175	0.841
5	2.51	0.14	0.100	0.093	0.669	0.132	0.957
6	2.24	0.12	0.116	0.097	0.786	0.124	1.00
7	1.57	0.09	0.102	0.072	0.833	0.087	1.00
8	1.36	0.08	0.091				

<sup>a</sup> Singular values from the SVD analysis of the eight datasets. <sup>b</sup> Root mean squared magnitude for each OLC dataset. <sup>c</sup> Root mean squared deviation between complete OLC data sets and all single-deletion OLC datasets. <sup>d</sup>  $Q^* = \text{RMSD}/\|D\|$ . <sup>e</sup> Maximum RMSD observed between the full OLC dataset and an individual deletion OLC dataset. <sup>f</sup>  $Q^*(\text{max}) = [\text{RMSD}(j)](\text{max})/\|D\|$ .

to data collection. Thus, asymmetric electrostatic interactions from the highly negatively charged phage rods combined with the prolate ellipsoidal steric effects from the strained polyacrylamide are combined along different directions in space, leading to a range of alignment tensors. Additional modulation of the alignment tensor can sometimes be obtained by varying the phage concentration or by the addition of magnesium ions.

Backbone amide  $^{15}\text{N}$ – $^1\text{H}$  RDCs were collected from  $\Delta 131\Delta$  in 4 M urea for a total of eight RDC data sets. Seven of these sets utilized composite Pf1/gels: a mixture of 3 and 10 mg/mL Pf1 phage concentrations with 6% polyacrylamide (19:1 acrylamide/bisacrylamide) at 0, 30, 55, and 90° relative to  $B_0$ . The eighth dataset was from a 6% gel that did not contain Pf1 phage. The RDCs were acquired using the  $[^{15}\text{N}, ^1\text{H}]$ -IPAP HSQC experiment and analyzed by singular value decomposition (SVD) to determine the number of independent alignment tensors present in the data. On the basis of the resultant singular values and propagated error estimates (Table 1), it is clear that there are at least three independent alignment tensors. These three independent RDC datasets can be reconstituted as linear combinations of the eight actually recorded RDC datasets (Supporting Information). These orthogonal linear combination (OLC)-RDC datasets correspond to the ideally independent RDCs that would be measured in  $\Delta 131\Delta$  if alignment tensors coincided with their respective principal axes. Correlation plots between the three most significant OLC datasets are shown in Figure 1, plots A–C.

An obvious concern is whether the second and third independent OLC-RDC datasets arise predominantly due to the presence of systematic errors or media-induced perturbations of the unfolded ensemble. Such effects, if they exist, would be expected to show a pronounced dependence on a specific experimentally recorded RDC dataset. To address this concern, an SVD analysis was carried out for subsets of the experimental RDC data in which single RDC datasets were deleted. After the systematic deletion of an experi-

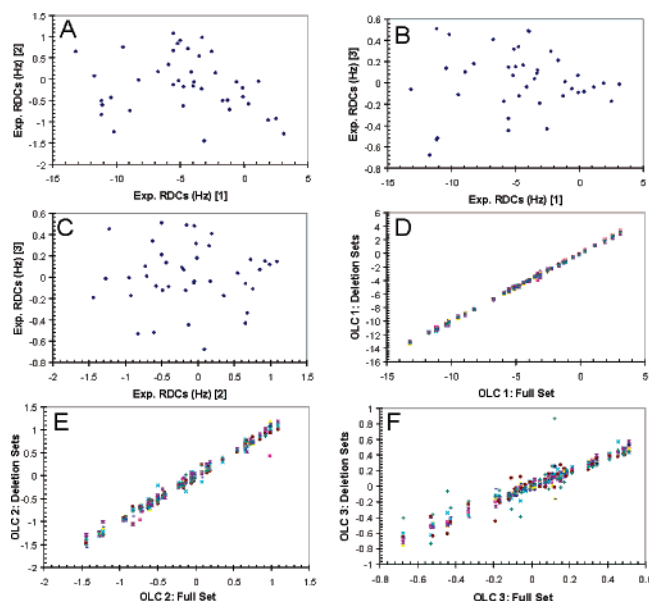


**Figure 1.** (A–C) Correlation plots of the three most significant orthogonal RDC datasets resulting from a SVD analysis of all data acquired using eight alignment media. (D–F) Correlation plots of the three most significant full OLC datasets against all corresponding single-deletion OLC datasets.

mental RDC dataset, the OLC-RDC datasets were redetermined by SVD and then compared to the original OLC-RDC datasets calculated using all eight measured RDC datasets. One would expect that if the content of a given OLC-RDC dataset corresponds to real signal as opposed to random or uncorrelated systematic errors, then it should remain relatively invariant to the removal of any one of the experimental RDC datasets from which it is constituted.

To quantify these results we define a statistic,  $Q^*$ , based on the ratio of the RMSD variation among deletion OLC-RDC datasets to the RMS magnitude of the relevant OLC-RDC dataset. Low values of  $Q^*$  indicate that the specific OLC-RDC dataset exhibits variations upon a single-set deletion which are small relative to the overall magnitude of the OLC-RDCs. For OLC-RDC datasets which are predominantly constituted of random noise, the value of  $Q^*$  will approach a value of 1. To monitor the possibility that a single errant RDC dataset accounts solely for the significance of a particular OLC-RDC dataset, the maximum  $Q^*$  value,  $Q^*(\max)$ , observed among all deletions is also reported. The results of this validation analysis are shown in Table 1 and plots of the deletion OLC-RDCs versus the three most significant full OLC-RDCs are shown in Figure 1D–F. Clearly, the first, second, and third OLC-RDC datasets are highly robust to the removal of any single experimental RDC dataset, establishing the presence of three independent alignment tensors among the collective RDC datasets measured for  $\Delta 131\Delta$ , sampled well above the level of experimental uncertainty. In addition to the present application, the above approach could be used to validate the existence of independent alignment tensors for cases in which structural information is unknown or of low resolution.

The observation that the RDC data span three or more dimensions of the five-dimensional parameter space demonstrates that the ensemble average structure of denatured nuclease must be asymmetric with respect to these three orthogonal principal axes. Along the first axis, which corresponds closely to the major steric axis, RDCs are skewed in sign, suggesting that amide bond vectors on average have an excess alignment either along or perpendicular to this axis. As proposed by others, this could be explained by an excess of extended conformations oriented with the long axis. However, along the second and third axes, which are orthogonal to the first and to each other, no such skewing of RDCs is observed, suggesting that the amide bond vector orientation lacks directional preference with respect to these axes. The dominant contribution made by the first alignment to any individual RDC dataset and the corresponding skewing of the RDC distribution lends support to the existence of an excess of extended conformations in the unfolded state. However, the measurement of RDCs corresponding to an additional two independent alignments now provides a more refined view, indicating that a specific tertiary structural arrangement, not inconsistent with a natelike topology, also persists in the denatured state. Since the mechanisms of electrostatic alignment require an asymmetric distribution of ionizable groups, either on the surface where they mediate transient binding or globally as described by a multipole expansion,<sup>13</sup> these data demonstrate an asymmetry in the distribution of charged residues, in addition to an asymmetry in the distribution of bond vectors. From the observed ensemble-averaged distribution of backbone orientations, one can view a denatured protein as spanning three-dimensional space with a large heterogeneous distribution of conformations yet unable to access all possible segment orientations.

**Supporting Information Available:** Construction of OLC-RDC dataset and definition of  $Q^*$ ; experimental RDCs from eight alignment media. This material is available free of charge via the Internet at <http://pubs.acs.org>.

## References

- (1) Shortle, D.; Ackerman, M. S. *Science* **2001**, *293*, 487–489.
- (2) Ding, K.; Louis, J. M.; Gronenborn, A. M. *J. Mol. Biol.* **2004**, *335*, 1299–1307.
- (3) Fieber, W.; Kristjansdottir, S.; Poulsen, F. M. *J. Mol. Biol.* **2004**, *339*, 1191–1199.
- (4) Mohana-Borges, R.; Goto, N. K.; Kroon, J. A. G.; Dyson, J. H.; Wright, P. E. *J. Mol. Biol.* **2004**, *340*, 1131–1142.
- (5) Louhivuori, M.; Fredriksson, K.; Paakkonen, K.; Permi, P.; Annala, A. *J. Biomol. NMR* **2004**, *29*, 517–524.
- (6) Gillespie, J. R.; Shortle, D. *J. Mol. Biol.* **1997**, *268*, 170–184.
- (7) Jha, A. K.; Colubri, A.; Free, K. F.; Sosnick, T. R. *Proc. Natl. Acad. Sci. U.S.A.* **2005**, *102*, 13099–13104.
- (8) Bernado, P.; Bertoncini, C. W.; Griesinger, C.; Zweckstetter, M.; Blackledge, M. *J. Am. Chem. Soc.* **2005**, *127*, 17968–17969.
- (9) Tolman, J. R. *J. Am. Chem. Soc.* **2002**, *124*, 12020–12031.
- (10) Meiler, J.; Peti, W.; Griesinger, C. *J. Am. Chem. Soc.* **2003**, *125*, 8072–8073.
- (11) Briggman, K. B.; Tolman, J. R. *J. Am. Chem. Soc.* **2003**, *125*, 10164–10165.
- (12) Ruan, K.; Tolman, J. R. *J. Am. Chem. Soc.* **2005**, *127*, 15032–15033.
- (13) Zweckstetter, M.; Hummer, G.; Bax, A. *Biophys. J.* **2004**, *86*, 3444–3460.

JA0627693